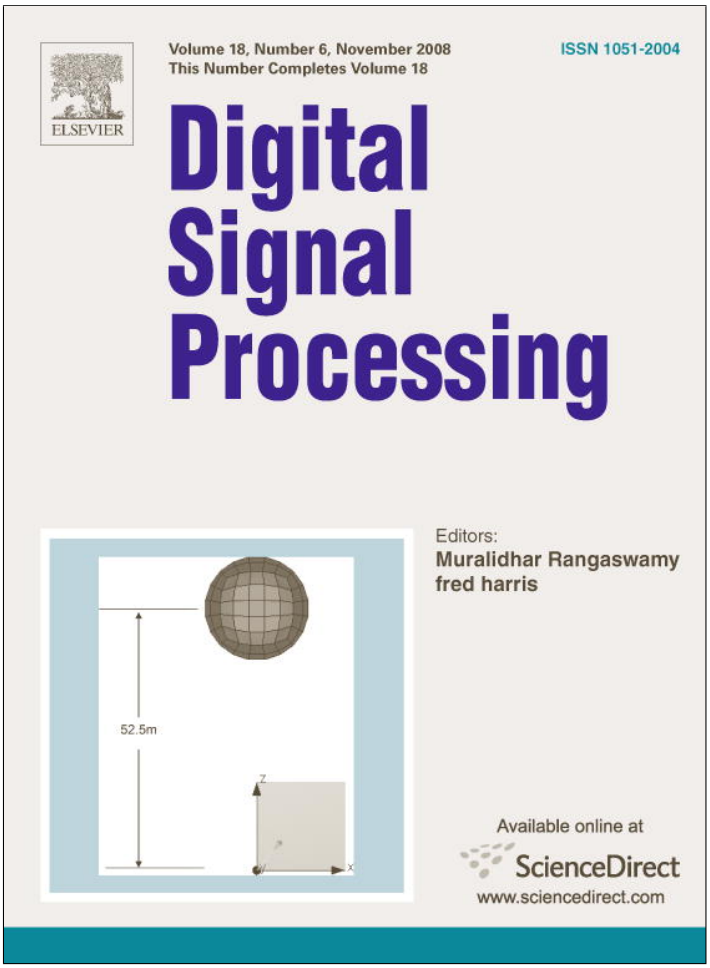

Digital Signal Processing 18 (2008) 907–918

Contents lists available at ScienceDirect

Digital Signal Processing

www.elsevier.com/locate/dsp

A high performance parallel Radon based OFDM transceiver design and simulation

Waleed Al-Jawhar [a], Abbas Hasan Kattoush [a,*], Sulaiman M. Abbas [b], Ali T. Shaheen [b]

[a] EE Engineering Department, Al-Isra University, Jordan
[b] EE Department, Baghdad University, Iraq

ARTICLE INFO

Article history:
Available online 26 April 2008

Keywords:
Finite Radon transform
Radon based OFDM
FRAT mapping
2-D ISI channel

ABSTRACT

A major goal of the next-generation wireless communication systems is the development of a reliable high-speed wireless communication system that supports high user mobility. They must focus on increasing the link throughput and the network capacity. In this paper a novel, spectral efficient system is proposed for generating and transmitting two-dimensional (2-D) orthogonal frequency division multiplexing (OFDM) symbols through 2-D inter-symbol interference (ISI) channel. Instead of conventional data mapping techniques, discrete finite Radon transform (FRAT) is used as a data mapping technique due to the increased orthogonality offered. As a result, the proposed structure gives a significant improvement in bit error rate (BER) performance. The new structure was tested and a comparison of performance for serial one-dimensional (1-D) Radon based OFDM and parallel 2-D Radon based OFDM is made under additive white Gaussian noise (AWGN), flat, and multi-path selective fading channels conditions. It is found that Radon based parallel 2-D OFDM has better speed and performance than serial 1-D Radon based OFDM.

1. Introduction

A major goal of modern communications is the development of a reliable high-speed wireless communication system that supports high user mobility. The next generation of wireless systems will require higher data quality than current cellular mobile radio systems and should provide higher bit rate services. In other words, the next generation of wireless systems are supposed to have a better quality and coverage, be more powerful and bandwidth efficient, and be deployed in diverse environments [1]. The ever-increasing demand for wireless and multimedia applications such as video streaming keeps pushing future wireless LAN (WLAN) systems to support much higher data rates (100 MB/s up to 1 GB/s) at high link reliability and over greater distances. Next-generation wireless communication systems are focused on increasing the link throughput (bit rate), the network capacity, and the transmit range [2]. A multi-band orthogonal frequency division multiplexing ultra wideband system is being considered for the physical layer of the new IEEE wireless personal area network (WPAN) standard, IEEE 802.15.3a [3,4]. The standard is targeting high data transmission rates of 110 Mb/s over 10 m, 220 Mb/s over 4 m and 480 Mb/s over 1 m. The IEEE 802.15.3a transceivers will be used in portable devices, such as camcorders, and laptops, as well as in fixed devices, such as TVs and desktops. Therefore the link throughput (bit rate), the network capacity and bandwidth efficiency are very important issues to be addressed.

OFDM system is one of the most promising technologies for current and future wireless communications [5]. It is a form of multi-carrier modulation (MCM) technologies [6–8] where data bits are encoded to multiple sub-carriers, while being

* Corresponding author.
E-mail address: akattoush@gmail.com (A.H. Kattoush).

1051-2004/$ – see front matter
doi:10.1016/j.dsp.2008.04.008

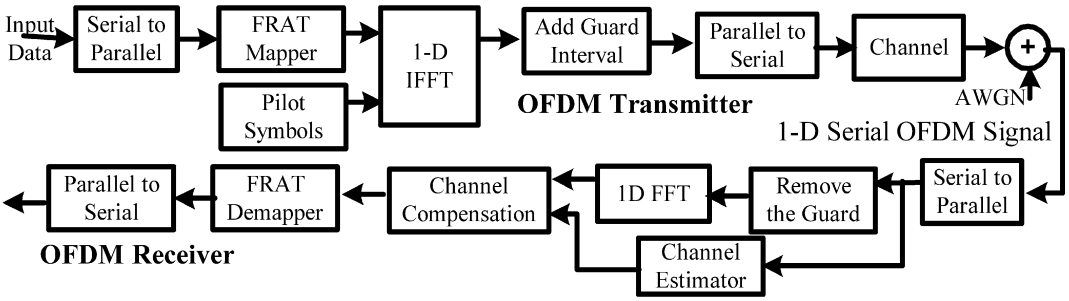

Fig. 1. Radon based serial OFDM transceiver.

sent simultaneously. Each sub-carrier in an OFDM system is modulated in amplitude and phase by the data bits. Modulation techniques typically used are binary phase shift keying (BPSK), quadrature phase shift Keying (QPSK), 16 quadrature amplitude modulation (QAM), 64QAM, etc. The process of combining different sub-carriers to form a composite time-domain signal is usually achieved using fast Fourier transform (FFT) and inverse FFT (IFFT) operations [9,10].

The main problem in the design of a communications system over a wireless link is to deal with multi-path fading, which causes a significant degradation in terms of both the reliability of the link and the data rate [11]. Multi-path fading channels have a severe effect on the performance of wireless communication systems even those systems that exhibits efficient bandwidth, like OFDM [12].

There is always a need for developments in the realization of these systems as well as efficient channel estimation and equalization methods to enable these systems to reach their maximum performance [13,14]. The OFDM receiver structure allows relatively straightforward signal processing to combat channel delay spreads, which was a prime motivation to use OFDM modulation methods in several standards, for example, digital audio/video broadcasting [15], wireless local area network (WLAN, IEEE 802.11a/g) [16], IEEE wireless personal area network (WPAN) standard IEEE 802.15.3a [3,4], IEEE 802.16 [17], digital audio/video broadcasting (DAB/DVB) [15], HiperLAN/2 [18], asymmetric DSL (ADSL), and very-high-speed DSL (VDSL) systems [19]. Also multi-band OFDM is a strong candidate for multi-band ultra wideband (UWB) which enables high data rate UWB transmission to inherit all the strength of OFDM that is widely used in numerous communication situations [20].

In transmissions over a radio channel, the orthogonality of the signals is maintained only if the channel is flat and time-invariant, channels with a Doppler spread and the corresponding time variations corrupt the orthogonality of the OFDM sub-carrier waveforms [21]. In a dispersive channel, self-interference occurs among successive symbols at the same sub-carrier casing ISI, as well as among signals at different sub-carriers casing ICI. It is well known that the FFT-based OFDM obtain the required orthogonality between the sub-carriers from the suitability of the IFFT algorithm [9]. This suitability makes the FRAT appropriate when used as a data mapping in the OFDM structure since it depends on the IFFT to obtain the required mapping. This increases the orthogonality of the system since IFFT is used twice, first in data mapping then in sub-channel modulation.

The Radon transform is the underlying fundamental concept used for computerized tomography scanning, as well for a wide range of other disciplines, including radar imaging, geophysical imaging, nondestructive testing, and medical imaging [22]. The enormous growth in the application areas of the Radon transform and the fact that digital computations are often required, has led to the development of the discrete Radon transform (DRT). The Radon transform (RT) is a widely studied algorithm used to perform image pattern extraction in fields such as computer graphics and several others digital signal and image processing applications [23–32].

A new application for FRAT is proposed in this paper. It is used as a mapping technique in OFDM realization in a new proposed 2-D OFDM system.

2. Radon based OFDM

In 1-D serial Radon based OFDM system, FRAT mapping is used instead of QAM mapping as shown in Fig. 1. The other processing parts of the system remain the same as in conventional QAM OFDM system. It is known that FFT-based OFDM obtain the required orthogonality between sub-carriers from the suitability of IFFT algorithm [9]. Using FRAT mapping with the OFDM structure increases the orthogonality between sub-carriers since FRAT computation uses 1-D IFFT algorithm. So 1-D serial Radon based OFDM system has increased orthogonality since 1-D IFFT algorithm is used twice: in data mapping and in sub-channel modulation, which is reflected in overall system performance. Sub-carriers are generated using N points discrete Fourier transform (DFT) and guard interval (GI) inserted at start of each symbol is used to reduce ISI. It may be zero-padded GI, cyclic prefix, or possibly other types of guard intervals. One possible type of GI is a half guard period, which is a cyclic prefix type in one half, and a zero padded in the other half.

Fig. 2 shows the guard interval as cyclic prefix in the serial 1-D OFDM. It is a copy of partial wave from the end of OFDM symbol. As in QAM OFDM, all symbols in this model are transmitted serially throw the 1-D channel. The channel is simulated as 1-D FIR filter that adds multi-path effect and AWGN to transmitted symbols. Channel estimator is used to estimate the channel effect.

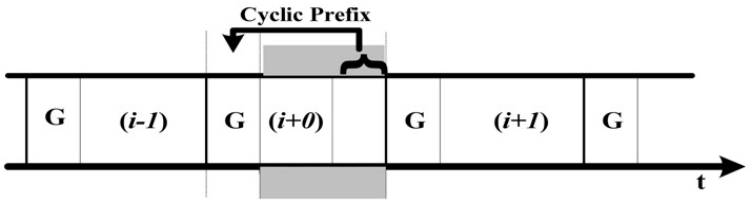

Fig. 2. Guard interval as cyclic prefix in the serial OFDM.

FRAT is proposed as a modulation mapping in the communication system and it is designed to increase the spectral efficiency of the OFDM system through increasing the bit per Hertz of the mapping. The procedure steps of using the 1-D serial Radon based OFDM mapping is as follows:

Step 1. Suppose $d(k)$ is the serial data stream to be transmitted using OFDM modulation scheme. Converting $d(k)$ from serial form to parallel form will construct a one-dimensional vector containing the data symbols to be transmitted,

$$d(k) = (d_0 d_1 d_2 \dots d_n)^T, \tag{1}$$

where k and n are the time index and the vector length, respectively.

Step 2. Convert the data packet represented by the vector $d(k)$ from one-dimensional vector to a $p \times p$ two-dimensional matrix $D(k)$, where p should be a prime number according to the matrix resize operation.

Step 3. Take the 2-D FFT of the matrix $D(k)$ to obtain the matrix, $F(r, s)$. For simplicity it will be labeled by F.

$$F(r,s) = \sum_{m=0}^{p-1} \sum_{n=0}^{p-1} D(m,n) e^{-j(2\pi/p)rm} e^{-j(2\pi/p)ns}. \tag{2}$$

Step 4. Redistribute the elements of the matrix F according to the optimum ordering algorithm given in [33]. So, the dimensions of the resultant matrix will be $p \times (p+1)$ and will be denoted by the symbol $\mathcal{F}_{\text{opt}}$. The two matrixes for FRAT window $= 7$ are given by

$$\mathcal{F} = \begin{bmatrix} f_1 & f_8 & f_{15} & f_{22} & f_{29} & f_{36} & f_{43} \\ f_2 & f_9 & f_{16} & f_{23} & f_{30} & f_{37} & f_{44} \\ f_3 & f_{10} & f_{17} & f_{24} & f_{31} & f_{38} & f_{45} \\ f_4 & f_{11} & f_{18} & f_{25} & f_{32} & f_{39} & f_{46} \\ f_5 & f_{12} & f_{19} & f_{26} & f_{33} & f_{40} & f_{47} \\ f_6 & f_{13} & f_{20} & f_{27} & f_{34} & f_{41} & f_{48} \\ f_7 & f_{14} & f_{21} & f_{28} & f_{35} & f_{42} & f_{49} \end{bmatrix}, \tag{3}$$

$$\mathcal{F}_{\text{opt}} = \begin{bmatrix} f_1 & f_1 & f_1 & f_1 & f_1 & f_1 & f_1 & f_1 \\ f_2 & f_{10} & f_9 & f_{16} & f_8 & f_{21} & f_{14} & f_{13} \\ f_3 & f_{19} & f_{17} & f_{31} & f_{15} & f_{34} & f_{20} & f_{18} \\ f_4 & f_{28} & f_{25} & f_{46} & f_{22} & f_{47} & f_{26} & f_{23} \\ f_5 & f_{30} & f_{33} & f_{12} & f_{29} & f_{11} & f_{32} & f_{35} \\ f_6 & f_{39} & f_{41} & f_{27} & f_{36} & f_{24} & f_{38} & f_{40} \\ f_7 & f_{48} & f_{49} & f_{42} & f_{43} & f_{37} & f_{44} & f_{45} \end{bmatrix}. \tag{4}$$

Step 5. Take the 1D-IFFT for each column of the matrix $\mathcal{F}_{\text{opt}}$ to obtain the matrix of Radon coefficients, R:

$$R = \frac{1}{p} \sum_{k=0}^{N-1} F_{\text{opt}} e^{\frac{j2\pi kn}{p}}. \tag{5}$$

Step 6. Construct the complex matrix $\overline{R}$ from the real matrix R such that its dimensions will be $p \times (p+1)/2$ according to

$$\overline{r_{l,m}} = r_{i,j} + j r_{i,j+1}, \quad 0 \leqslant i \leqslant p, \ 0 \leqslant j \leqslant p, \tag{6}$$

where $\overline{r_{l,m}}$ refers to the elements of the matrix $\overline{R}$, while $r_{i,j}$ refers to the elements of the matrix R. Matrixes R and $\overline{R}$ are given by

$$\mathcal{R} = \begin{bmatrix} r_{1,1} & r_{1,2} & r_{1,3} & \dots & r_{1,p+1} \\ r_{2,1} & r_{2,2} & r_{2,3} & \dots & r_{2,p+1} \\ \vdots & \vdots & \vdots & \dots & \vdots \\ \vdots & \vdots & \vdots & \dots & \vdots \\ r_{p-1,1} & r_{p-1,2} & r_{p-1,3} & \dots & r_{p-1,p+1} \\ r_{p,1} & r_{p,2} & r_{p,3} & \dots & r_{p,p+1} \end{bmatrix}, \tag{7}$$

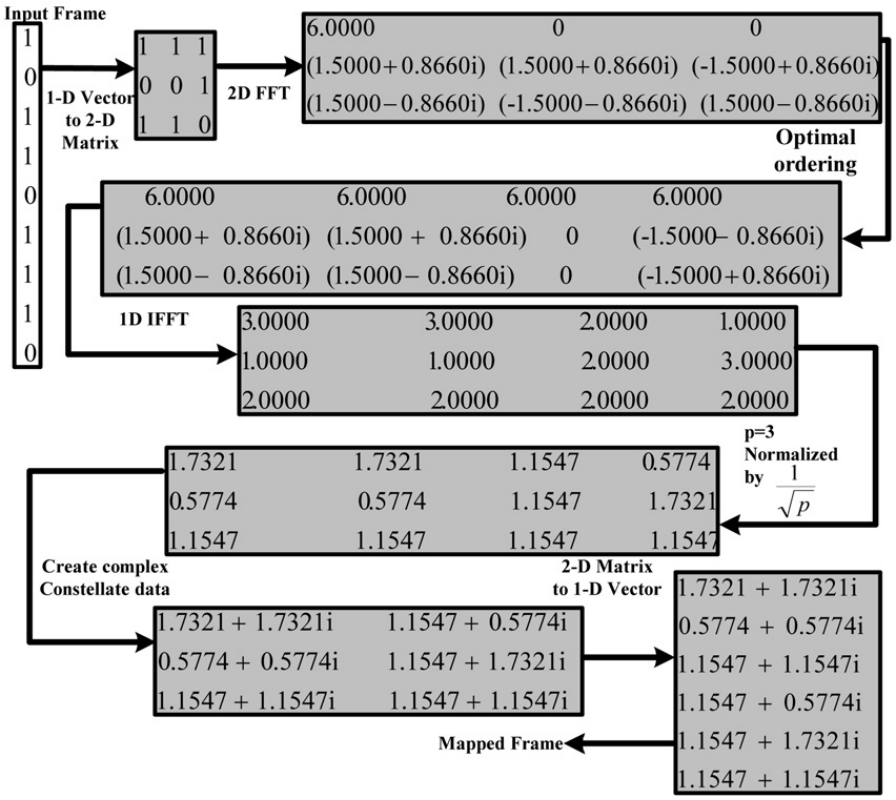

Fig. 3. An illustrative numerical example of converting binary data to constellated data using FRAT mapping.

$$\bar{\mathcal{R}} = \begin{bmatrix} r_{1,1} + jr_{1,2} & r_{1,3} + jr_{1,4} & \cdots & r_{1,p} + jr_{1,p+1} \\ r_{2,1} + jr_{2,2} & r_{2,3} + jr_{2,4} & \cdots & r_{2,p} + jr_{2,p+1} \\ \vdots & \vdots & \cdots & \vdots \\ \vdots & \vdots & & \vdots \\ \vdots & \vdots & \cdots & \vdots \\ r_{p-1,1} + jr_{p-1,2} & \cdots & \cdots & r_{p-1,p} + jr_{p-1,p+1} \\ r_{p,1} + jr_{p,2} & \cdots & \cdots & r_{p,p} + jr_{p,p+1} \end{bmatrix}. \tag{8}$$

Step 7. Resize the matrix $\bar{R}$ to a one-dimensional vector $r(k)$ of length $p \times (p+1)/2$.

$$r(k) = (r_0 \quad r_1 \quad r_2 \quad \ldots \quad r_{p(p+1)/2})^T. \tag{9}$$

Step 8. Take the 1D-IFFT for the vector, $r(k)$ to obtain the sub-channel modulation.

$$s(k) = \frac{1}{p(p+1)/2} \sum_{k=0}^{N_C-1} r(k) e^{\frac{j2\pi kn}{p(p+1)/2}}, \tag{10}$$

where N_C number of carriers.

Step 9. Finally, convert the vector $s(k)$ to serial data symbols: $s_0, s_1, s_2, \ldots, s_n$.

An illustrative numerical example of converting binary data to constellated data using FRAT mapping is shown in Fig. 3.

3. Two-dimensional channel model

Two-dimensional finite state input channels with memory play a fundamental role in various applications in modern communications. A popular and important instance of this class of channels is 2-D ISI channels, which appear, e.g., in magnetic and optical recording systems [34,35]. In ISI, finite state symbols are ordered on a 2-D grid, causing interference in a limited neighborhood. Another interesting instance of dispersive 2-D channels is multiple-access (MA) channels, which appear in cellular networks. Following Wyner's cellular model [36], a planar uplink model can be viewed as a 2-D channel, where each cell corresponds to a node in the grid, and interference occurs between neighboring cells. This Wyner-like model assumes that most of the multiple-access interference (MAI) is caused by inter-cell effects, rather than intra-cell effects.

Many researchers have proposed 2-D ISI channel detection schemes models, [34,35,37–42]. Singla et al. have proposed joint equalization and decoding schemes for 2-D ISI discrete channels, and this is the channel model used in this paper for

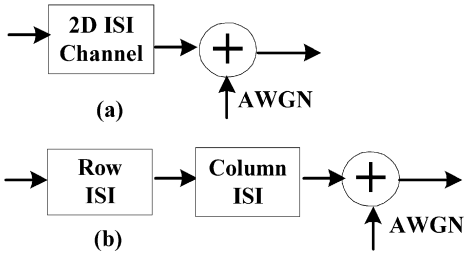

Fig. 4. Two-dimensional ISI channels. (a) Nonseparable channel, (b) separable channel.

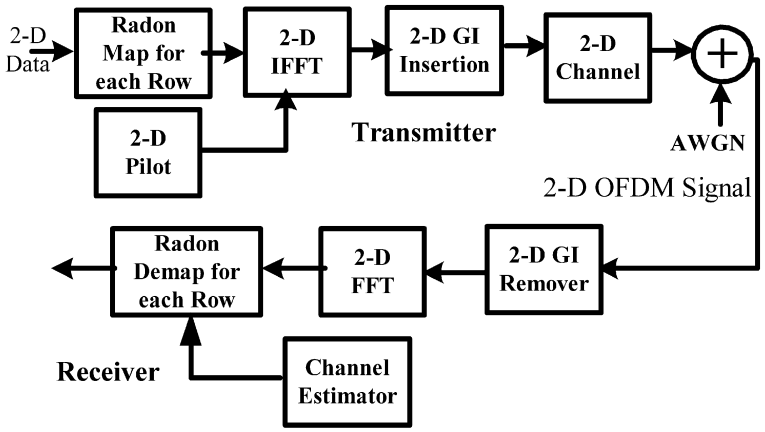

Fig. 5. The proposed parallel Radon based OFDM system.

simulation of the proposed 2-D parallel OFDM system. This channel model is a binary-input, liner finite-state ISI channel where the input to this channel is 2-D matrix of size $(L_1 \times L_2)$. The output of this channel is described by

$$r(i,j) = \sum_{k_1,k_2=0}^{L1,L2} x(i-k_1, j-k_2)h(k_1,k_2) + w(i,j), \tag{11}$$

where $r(i,j)$ and $x(i,j)$ are elements of output and input data matrices respectively; $w(i,j)$ are samples of additive white Gaussian noise (AWGN) with variance σ^2; h is the 2-D channel impulse response:

$$h = \begin{bmatrix} h_0 & h_1 \\ h_2 & h_3 \end{bmatrix}. \tag{12}$$

For example, an impulse response used in simulation in [37] is

$$h = \begin{bmatrix} 1 & 0.5 \\ 0.5 & 0.25 \end{bmatrix}.$$

This channel response is separable into $h = [1\ 0.5]^T[1\ 0.5]$.

In Eq. (11), L_1, L_2 represent number of elements over which ISI extends in each dimension. The channels impulse responses can be divided in to two types: non separable ISI channel and separable ISI channel as shown in Fig. 4.

4. Proposed parallel Radon based OFDM

The conventional and 1-D serial Radon based OFDM systems transmit data serially where proposed 2-D parallel Radon based OFDM system transmits data in parallel (transmitted signal is 2-D OFDM signal). This increases transmission speed, since parallel transmission is much faster than serial transmission and so this system is suitable for applications requiring high data rates. Proposed 2-D parallel Radon based OFDM system is shown in Fig. 5, it deals with 2-D input data of size $(M \times M)$. Each row of input data is represented by one 2-D OFDM symbol at the output of proposed system.

Proposed system will find a Radon map for each row and extend the 2-D matrix to IFFT size by adding zeros to the rows and columns. The matrix size after row and column zero padding will be of size $(N \times N)$. At the same time proposed system generates 2-D pilot carriers that assist channel estimator of size $(M \times M)$ and it also extend this 2-D pilot to $(N \times N)$. The second step in the system is generating the carriers by taking 2-D IFFT.

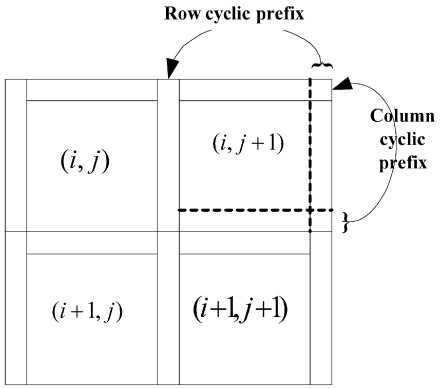

Fig. 6. Guard interval as cyclic prefix in the parallel OFDM.

If 2-D input data sequence is $a[k_1, k_2]$, where $0 \leqslant k_1 \leqslant N_1 - 1$ and $0 \leqslant k_2 \leqslant N_2 - 1$ and if frequency spacing Δf_1 raw wise and Δf_2 column wise, and if symbol intervals are Tu_1, Tu_2 raw wise and column wise, respectively, then transmitted signal can be written as

$$x(t_1, t_2) = \sum_{k_1=0}^{N_1-1} \sum_{k_2=0}^{N_2-1} a(k_1, k_2) e^{j2\pi k_1 \Delta f_1 t_1} e^{j2\pi k_2 \Delta f_2 t_2}, \quad 0 \leqslant t_1 \leqslant Tu_1 \text{ and } 0 \leqslant t_2 \leqslant Tu_2. \tag{13}$$

If the signal is sampled at rate Tu_1/N_1 row wise and Tu_2/N_2 column wise then

$$x_a(n_1, n_2) = x(n_1 Tu_1/N_1, n_2 Tu_2/N_2), \tag{14}$$

$$x_a(n_1, n_2) = \sum_{k_1=0}^{N_1-1} \sum_{k_2=0}^{N_2-1} a(k_1, k_2) e^{j2\pi k_1 n_1 \Delta f_1 Tu_1/N1} e^{j2\pi k_2 n_2 \Delta f_2 Tu_2/N2}. \tag{15}$$

If $\Delta f Tu = 1$, then

$$x_a(n_1, n_2) = \sum_{k_1=0}^{N1-1} \sum_{k_2=0}^{N2-1} a(k_1, k_2) e^{j2\pi k_1 n_1/N1} e^{j2\pi k_2 n_2/N2}, \tag{16}$$

$$x_a(n_1, n_2) = N_1 N_2 \times \big[\text{2-D IFFT}\{a(k)\}\big]. \tag{17}$$

The 2-D IFFT maintains orthogonality row wise and column wise, i.e., the contents of each row will be orthogonal and at the same time the contents of each column will be orthogonal too. That is the key property that allows this signal to be transmitted via 2-D ISI channel.

To reduce ISI in 2-D OFDM as in 1-D OFDM signal, the cyclic prefix can be added to the 2-D matrix, as shown in Fig. 6. A copy of partial end of each row is added to its start and a copy of partial end of each column end is added to its start. If the guard interval consists of k samples then the final 2-D matrix will be of size $(S \times S)$, where $S = N + k$. Adding GI to each row will reduce the ISI row and adding GI to each column will reduce ISI column.

Instead of using QAM mapping usually used with the standard FFT-based OFDM, the 1-D serial OFDM Radon mapping is used in the parallel 2-D OFDM system; this is due to its good suitability to OFDM structure because it depends on the 1D-IFFT to obtain the required mapping, which increases the orthogonality of the system since IFFT is used twice, first in data mapping and second in 2-D IFFT in the sub-channel modulation. In this paper the performance of 2-D parallel Radon based OFDM system is compared with that of 1-D serial Radon based OFDM. Using 2-D IFFT in carrier generation and using row and column zero padding in 2-D parallel OFDM gives better orthogonality and as a result better performance than 1-D serial OFDM.

5. Simulation and BER performance of proposed 2-D parallel Radon based OFDM transceiver

The simulation is started for 1-D serial Radon based OFDM system, its BER performance is simulated and compared with the conventional standard FFT-based OFDM for AWGN, flat fading, and multi-path fading channels. The system parameters used through the simulations are: bit duration $T_d = 1$ μs, FRAT window is 7 by 7, FFT bins = 64, Guard interval: Cyclic prefix approach with 26 symbols are added to the frame with pilot assisted channel estimator. A second-ray is assumed in multi-path fading channel with a second path gain of -8 dB, at a maximum delay of $\tau_{max} = 1$ μs. The results of this simulation are provided in Figs. 7–9. Fig. 7 shows the BER performance of the 1-D Radon based OFDM and the standard FFT based OFDM simulated in AWGN channel. From which it can be seen that the 1-D Radon based OFDM has a gain of about 4 dB SNR as compared with the standard FFT based OFDM to achieve a BER performance of 10^{-4}. The simulation in

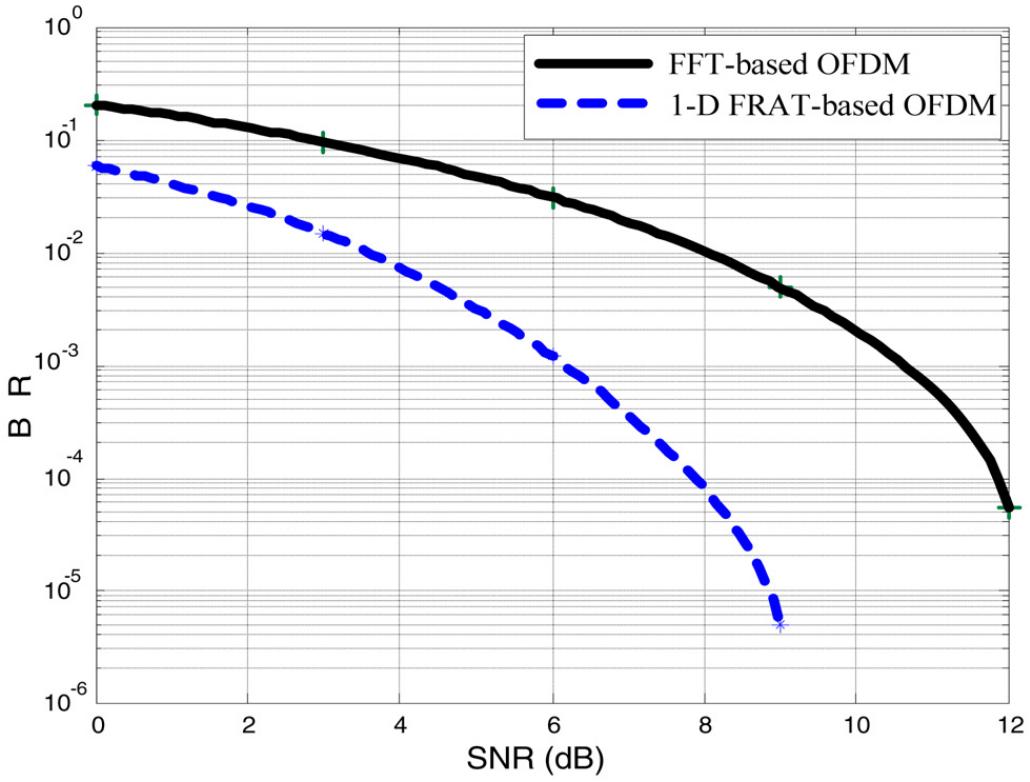

Fig. 7. BER performance of 1-D FRAT and FFT based OFDM in AWGN channel.

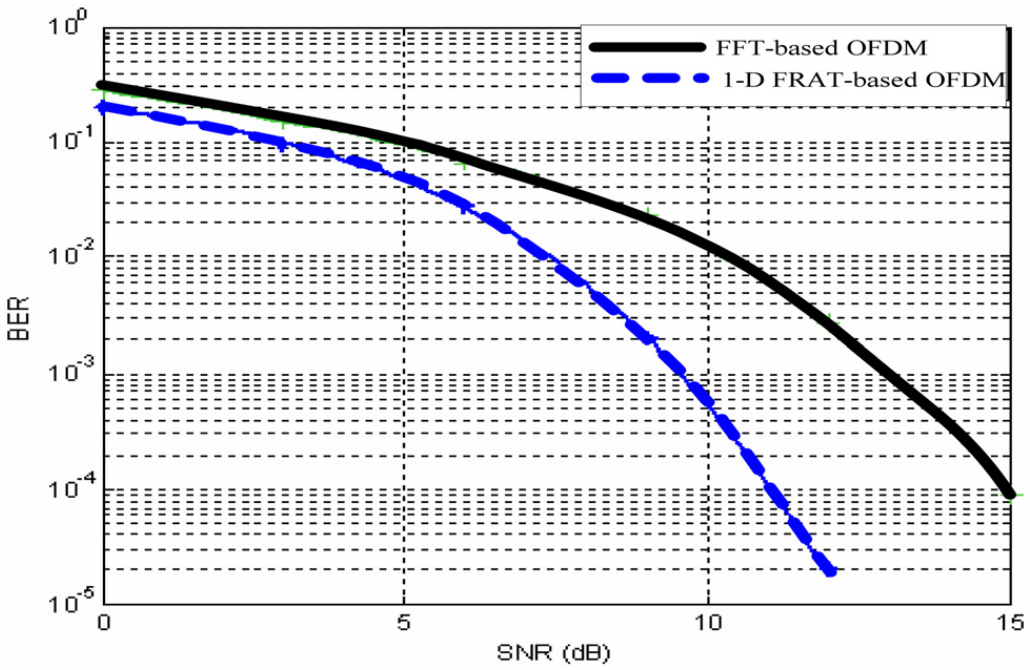

Fig. 8. BER performance of 1-D FRAT and FFT based OFDM in flat fading with AWGN channel.

a flat Raleigh-distributed fading channel with AWGN is given in Fig. 8. It shows that the Radon based OFDM has a gain in SNR of about 4 dB as compared with the standard FFT based OFDM to achieve a BER performance of 10^{-4}. Fig. 9 shows the BER performance of 1-D FRAT and FFT based OFDM in a 2-ray Rayleigh-distributed multi-path fading channel were the second path gain and delay was -8 dB and $\tau_{\max} = 1$ μs, respectively. It can be seen that BER performance of the Radon based OFDM is still better than the standard FFT-based OFDM. It requires 24 dB of SNR for 1-D FRAT OFDM to reach BER of 10^{-4} while the standard FFT based does not achieve such a BER without more complex equalization.

Then the performance of the 2-D parallel Radon based OFDM system is compared with the performance of the 1-D serial Radon based OFDM. Systems parameters used in simulation are: FRAT window is 7 by 7 ($p = 7$), 2-D FFT bins $= (64 \times 64)$,

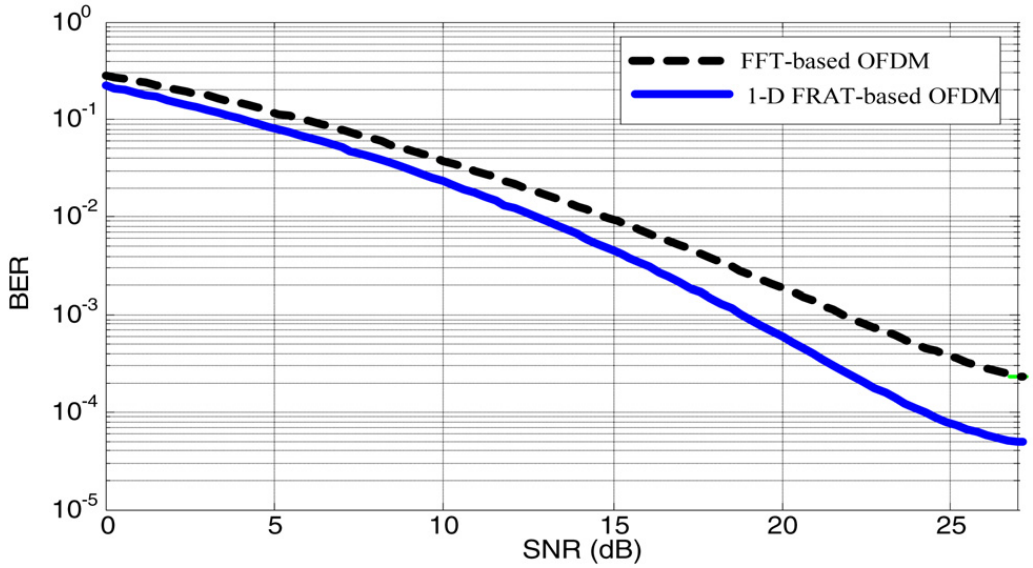

Fig. 9. BER Performance in frequency-selective fading channel.

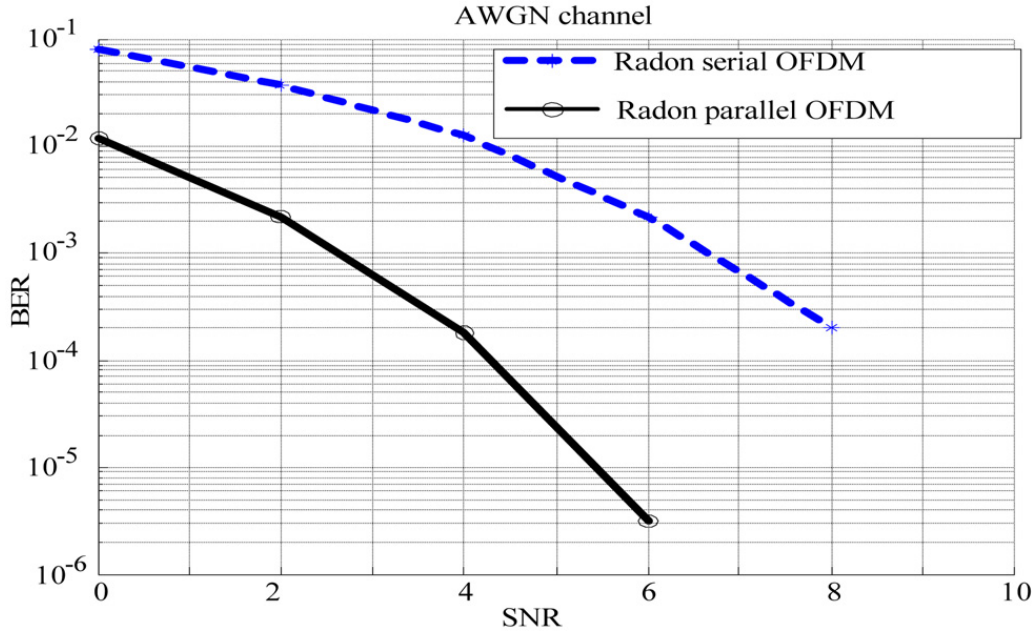

Fig. 10. BER for parallel Radon OFDM and serial Radon OFDM in AWGN channel.

guard interval = 16 samples row and column wise (1/4 × IFFT size), guard interval type equal all zeros, and 2-D pilot-assisted channel estimator is used in this simulation. Different types of channel models are used in the simulation. First an AWGN channel is considered with several signal-to-noise ratio (SNR) values. Then a multi-path Raleigh distributed fading channels are considered with two scenarios: flat and frequency selective fading (two path channel model) cases.

The channel impulse response used in the case of flat fading channel is

$$h = \begin{bmatrix} 1 & 0 \\ 0 & 0 \end{bmatrix}$$

and the channel impulse response used in the case of selective fading channel is

$$h = \begin{bmatrix} 1 & 0.5 \\ 0.5 & 0.25 \end{bmatrix}.$$

Fig. 10 shows BER performance of 2-D parallel Radon based OFDM compared with BER performance of 1-D serial Radon based OFDM in an AWGN channel. It can be seen from figure that parallel Radon OFDM has a gain in SNR about 5 dB to achieve a BER performance of 10^{-4} as compared with the 1-D serial Radon based OFDM.

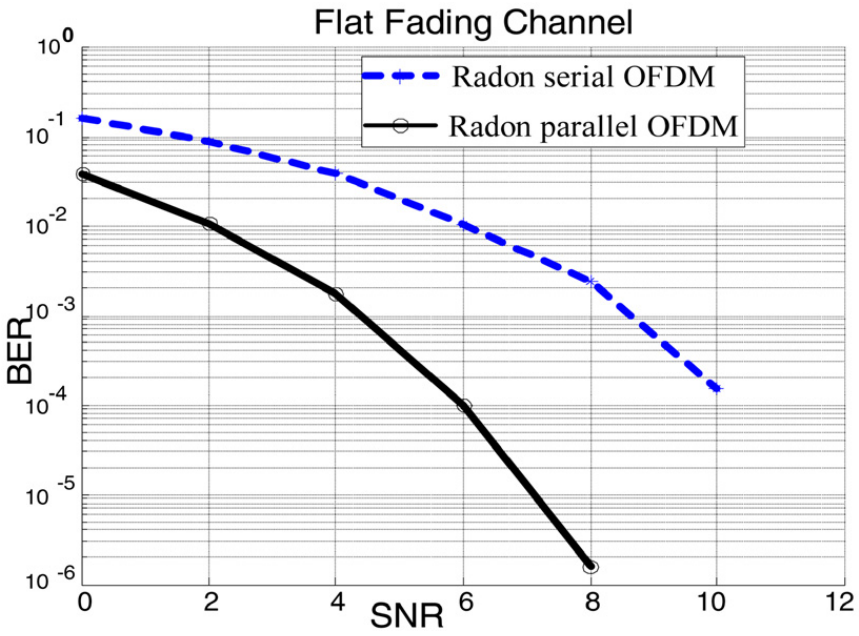

Fig. 11. BER for parallel and serial Radon based OFDM in flat fading channel.

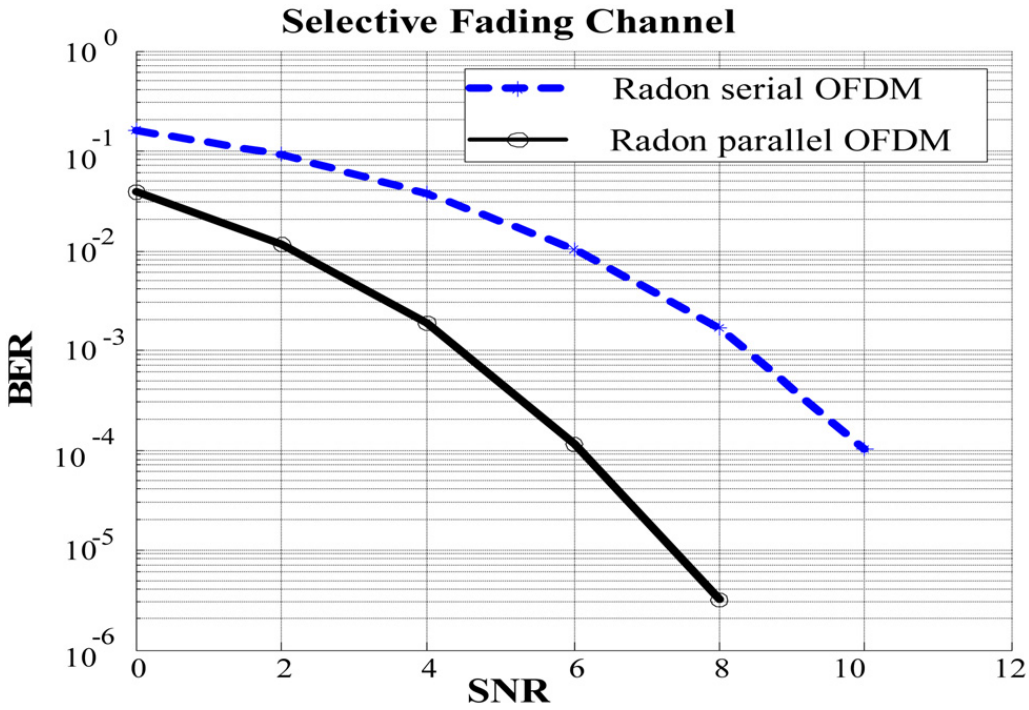

Fig. 12. BER for parallel and serial-Radon based OFDM in selective fading channel.

Fig. 11 plots BER performance of 2-D parallel Radon based OFDM compared with BER performance of 1-D serial Radon based OFDM in a flat fading channel. It can be noted that parallel Radon OFDM has a gain in SNR more than 4 dB to achieve a BER performance of 10^{-4} as compared with the 1-D serial Radon based OFDM.

Fig. 12 shows the BER performance of the two systems in selective fading channel with second path signal delay of 2 samples and gain equal to -10.5 dB. Simulations show that 2-D parallel Radon OFDM better performance in general and it has a gain improvement in SNR about 4 dB to achieve a BER performance of 10^{-4} as compared with the 1-D serial Radon based OFDM.

The effect of variations of second path gain and delay in static selective fading channel on the BER performance of the proposed 2-D system is studied. Fig. 13 depicts the effect of changing the second path gain on the BER performance as compared with 1-D Radon OFDM when the second path delay is two samples. The second path gains used are -8, -6, and -2 dB for row and column wise in the 2D ISI channel. From Fig. 13, it can be seen that the performance of the 2-D Radon based OFDM decreases with increasing second path gain, however it still better than that of the 1-D Radon based OFDM.

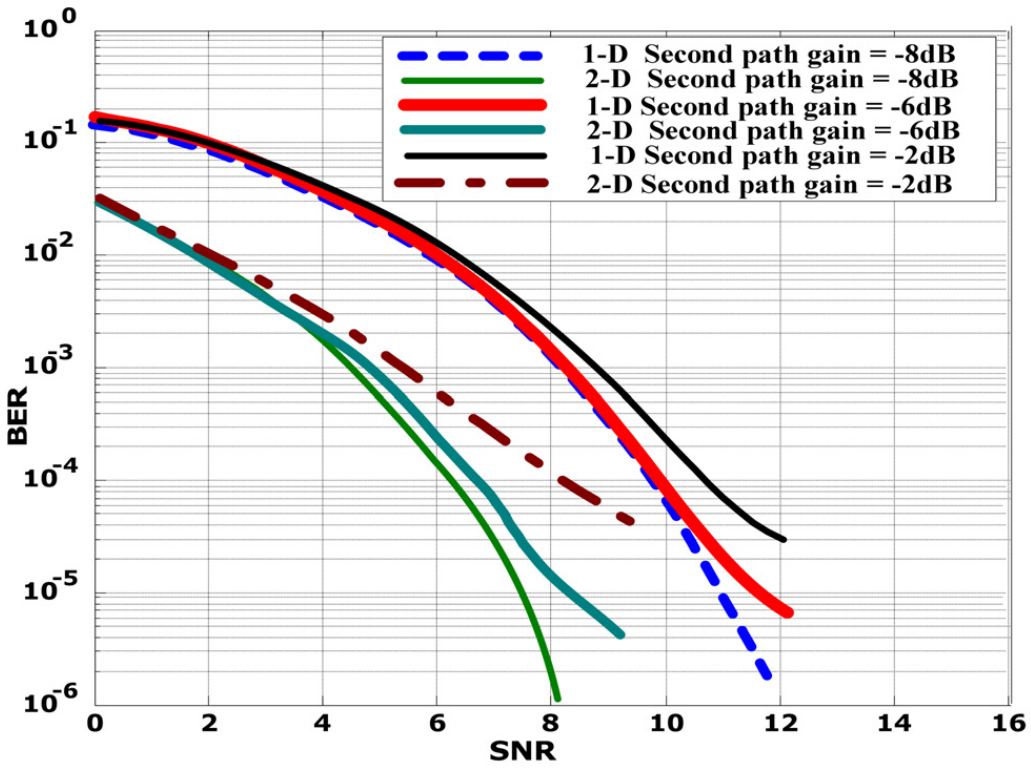

Fig. 13. Effect of second path gain on BER performance of the proposed parallel and serial-Radon based OFDM.

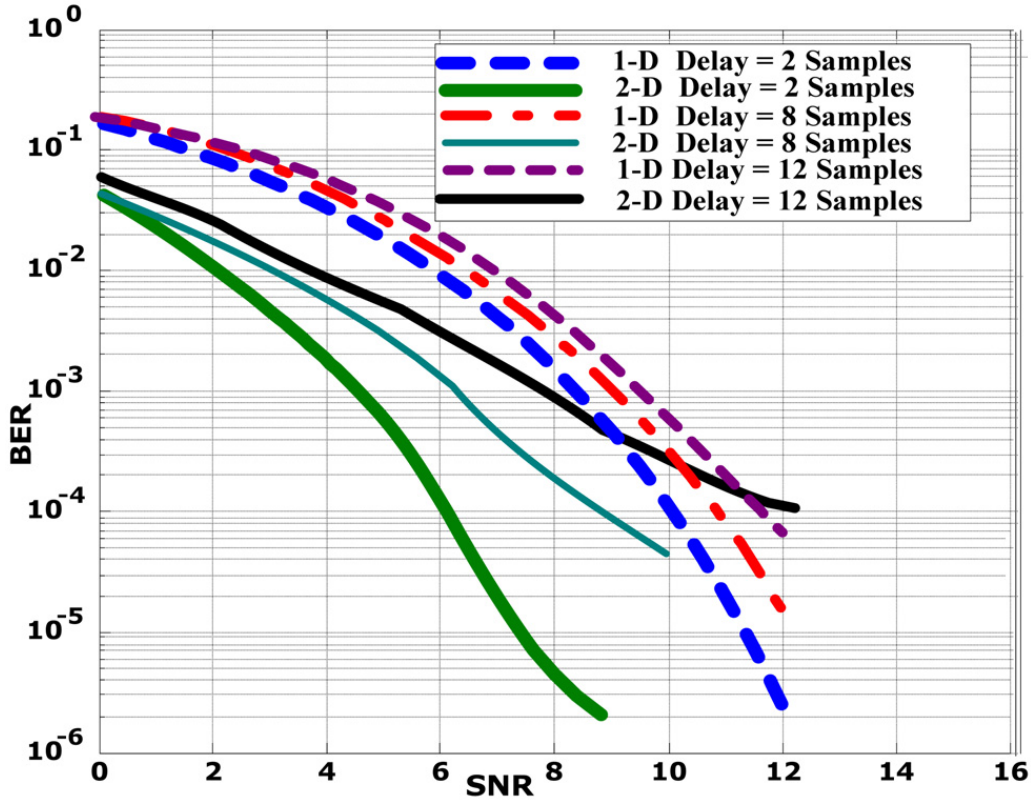

Fig. 14. Effect of second path delay on the BER performance of the proposed parallel and serial-Radon based OFDM.

Fig. 14 shows the effect of the second path delay on the Radon based 2-D OFDM as compared with that of Radon based 1-D OFDM when the second path gain is kept constant on −10 dB. The second path delays used are 2, 8, and 12 samples for row and column wise in the 2-D ISI channel. From Fig. 14 it can be seen that Radon based 2-D OFDM has better performance than that of Radon based 1-D OFDM.

6. Conclusions

In this paper a new OFDM generation method is proposed. This method generates 2-D OFDM symbols and transmits them through 2-D ISI channel. Using this method transmission speed is increased and therefore high data rate applications are easier to implement. The proposed 2-D parallel OFDM system uses Radon mapping instead of QAM mapping which increases the orthogonality. This method is easy to implement and it does not require complex processing. Simulation results of proposed 2-D parallel Radon based OFDM show a good SNR gain improvement compared with 1-D serial Radon OFDM in an AWGN, a flat fading, and a selective fading channel. The performance is improved in parallel system, due to implementation of IFFT twice, in data mapping and in 2-D IFFT in the sub-carrier modulation. Also the optimal ordering (best direction) in the Radon mapping can be considered as a good interleave which serves as an error spreading. The row and column zero padding before the 2-D IFFT and the use of 2-D channel estimator increases the system performance. Many techniques can be used as future work to increase system performance such as 2-D channel equalization, channel codes, and polynomial cancellation coding (PCC) algorithms.

References

[1] S.M. Alamouti, A simple transmit diversity technique for wireless communications, IEEE J. Select Area Commun. 16 (1998) 1451–1458.
[2] D.G. Rahn, M.S. Cavin, Fa Foster Dai, N.H.W. Fong, R. Griffith, J. Macedo, A.D. Moore, J.W.M. Rogers, M. Toner, A fully integrated multiband MIMO WLAN transceiver RFIC, IEEE J. Solid-State Circuits 40 (2005) 1629–1641.
[3] J. Foerster, Channel modeling sub-committee report final, Technical report, IEEE802.15-02/490, 2003.
[4] J. Balakrishnan, A. Batra, A. Dabak, A multi-band OFDM system for UWB communication, in: IEEE Conference on Ultra Wideband Systems and Technologies, 2003, pp. 354–358.
[5] O.-S. Shin, A.M. Chan, H.T. Kung, V. Tarokh, Design of an OFDM cooperative space-time diversity system, IEEE Trans. Vehic. Technol. 56 (2007) 2203–2215.
[6] I. Kalet, The multitone channel, IEEE Trans. Commun. 37 (1989) 119–124.
[7] N. Al-Dhahir, J.M. Cioffi, Optimum finite-length equalization for multicarrier transceivers, IEEE Trans. Commun. 44 (1996) 56–64.
[8] H. Zhang, D. Yuan, M. Pätzold, Novel study on PAPRs reduction in wavelet-based multicarrier modulation systems, Digital Signal Process. 17 (2007) 272–279.
[9] S. Weinstein, P. Ebert, Data transmission by frequency division multiplexing using the discrete Fourier transform, IEEE Trans. Commun. Technol. COM-19 (1971) 628–634.
[10] J.-C. Kuo, C.-H. Wen, C.-H. Lin, A.-Y. Wu, VLSI design of a variable-length FFT/IFFT processor for OFDM-based communication systems, EURASIP J. Appl. Signal Process. 13 (2003) 1306–1316.
[11] N.H. Tran, H.H. Nguyen, T. Le-Ngoc, Bit-interleaved coded OFDM with signal space diversity: Subcarrier grouping and rotation matrix design, IEEE Trans. Signal Process. 55 (2007) 1137–1149.
[12] E. Lawrey, The Suitability of OFDM as a modulation technique for wireless telecommunications, with a CDMA comparison, Thesis, James Cook University, October 1997.
[13] W.G. Jeon, K.H. Chang, Y.S. Cho, An equalization technique for orthogonal frequency-division multiplexing systems in time-variant multipath channels, IEEE Trans. Commun. 47 (1999) 27–32.
[14] X. Ma, H. Kobayashi, S.C. Schawrtz, EM-based channel estimation algorithms for OFDM, EURASIP J. Appl. Signal Process. 10 (2004) 1460–1477.
[15] R.V. Nee, R. Prasad, OFDM for Wireless Multimedia Communications, Artech House, London, 2000.
[16] IEEE, Part 11: Wireless LAN medium access control (MAC) and physical layer (PHY) specifications: High-speed physical layer in the 5 GHz band, September 1999, IEEE Std 802.11a-1999.
[17] I. Koffman, V. Roman, Broadband wireless access solutions based on OFDM access in IEEE 802.16, IEEE Commun. Mag. 40 (2002) 96–103.
[18] W.Y. Zou, Y. Wu, COFDM: An overview, IEEE Trans. Broadcast 41 (1995) 1–8.
[19] I. Lee, J.S. Chow, J.M. Cioffi, Performance evaluation of a fast computation algorithm for the DMT in high-speed subscriber loop, IEEE J. Select. Areas Commun. 13 (2007) 1564–1570.
[20] A. Batra, J. Balakrishnan, G.R. Aiello, J.R. Foerster, A. Dabak, Design of multiband OFDM system for realistic UWB channel environments, IEEE Trans. Microwave Theory Tech. 52 (2004) 2123–2138.
[21] L.J. Cimini Jr., Analysis and simulation of a digital mobile channel using orthogonal frequency division multiplexing, IEEE Trans. Commun. COM-33 (1985) 665–675.
[22] S.R. Deans, The Radon Transform and Some of Its Applications, Wiley, New York, 1983.
[23] K. Estabridis, R. Defigueiredo, Blood vessel detection via a multi-window parameter transform, in: Proceedings of the 19th IEEE Symposium on Computer-Based Medical Systems CBMS'06, IEEE Computer Society, 2006.
[24] K.G. van den Boogaart, R. Hielscher, J. Prestin, H. Schaeben, Kernel-based methods for inversion of the Radon transform on SO_3 and their applications to texture analysis, J. Comp. Appl. Math. 199 (2007) 122–140.
[25] Ph. Courmontagne, An improvement of ship wake detection based on the radon transform, Signal Process. 85 (2005) 1634–1654.
[26] A. Kingston, I. Svalbe, Geometric shape effects in redundant keys used to encrypt data transformed by finite discrete radon projections, in: Proceedings of the Digital Image Computing on Techniques and Applications DICTA'05, IEEE Computer Society, December 2005.
[27] D.A. Popov, D.V. Sushko, Image restoration in optical-acoustic tomography, Probl. Inform. Transmiss. 40 (2004) 254–278.
[28] M. Xu, L.-H.V. Wang, Time-domain reconstruction for thermo-acoustic tomography in a spherical geometry, IEEE Trans. Med. Imag. 21 (2002) 814–822.
[29] D. Zheng, Y. Liu, J. Zhao, A. El Saddik, A survey of RST invariant image watermarking algorithms, ACM Comp. Surveys (CSUR) 39 (2007) 1–91.
[30] J. Coetzer, B.M. Herbst, J.A. du Preez, Offline signature verification using the discrete radon transform and a hidden Markov model, EURASIP J. Appl. Signal Process. 2004 (2004) 559–571.
[31] X. Wang, B. Xiao, J.-F. Ma, X.-L. Bi, Scaling and rotation invariant analysis approach to object recognition based on Radon and Fourier–Mellin transforms, Pattern Recogn. 40 (2007) 3503–3508.
[32] T. Tsuboi, S. Hirai, Detection of planar motion objects using Radon transform and one-dimensional phase-only matched filtering, Syst. Comput. 37 (2006) 56–66.
[33] M.N. Do, M. Vetterli, The finite ridgelet transform for image representation, IEEE Trans. Image Process. 12 (2003) 16–28.
[34] P.S. Kumar, S. Roy, Two-dimensional equalization: Theory and application to high density magnetic recording, IEEE Trans. Commun. 42 (1994) 386–395.
[35] K.M. Chugg, X. Chen, M.A. Neifeld, Two-dimensional equalization in coherent and incoherent page-oriented optical memory, J. Opt. Soc. Amer. A 16 (1999) 549–562.

[36] A.D. Wyner, Shannon-theoretic approach to a Gaussian cellular multiple-access channel, IEEE Trans. Inform. Theory 40 (1994) 1713–1727.
[37] N. Singla, J.A. O'Sullivan, R.S. Indeck, Y. Wu, Iterative decoding and equalization for 2-D recording channels, IEEE Trans. Magn. 38 (2002) 2328–2330.
[38] Y. Wu, J.A. O'Sullivan, N. Singla, R.S. Indeck, Iterative detection and decoding for separable two-dimensional intersymbol interference, IEEE Trans. Magn. 39 (4) (2003) 2115–2120.
[39] M. Marrow, J.K. Wolf, Iterative detection of 2-dimensional channels, IEEE Info. Theory Workshop, Paris, France, March 2003.
[40] A. Moinian, L. Fagoonee, B. Honary, W. Coene, Linear channel model for multilevel two dimensional optical storage, in: Proc. 7th Int. Symp. Comm. Theory and Applications, Ambleside, Lake District, UK, July 2003, pp. 352–356.
[41] O. Shental, A.J. Weiss, N. Shental, Y. Weiss, Generalized belief propagation receiver for near-optimal detection of two-dimensional channels with memory, IEEE Info. Theory Workshop, San Antonio, Texas, October 2004.
[42] J. Wang, H. Zhou, Two-dimensional channel estimation based on sliding window for digital amplitude modulation broadcasting system, in: International Conference on Innovative Computing, Information and Control, vol. I, ICICIC'06, 2006, pp. 167–170.

Waleed Ameen Al-Jawher is a Dean of Engineering College, University of Isra, Jordan. He received a School of Research in digital signal processing in 2005, Ph.D. degree in digital signal processing from University of Wales University College of Swansea, United Kingdom, in 1986. He has a teaching experience in engineering for 32 years, a total of 15 National Awards. He published over 224 papers, supervised 202 M.Sc. and Ph.D. students. He was the first Professor Award of University of Baghdad, the first Professor Award of the Ministry of Higher Education and Scientific Research of Iraq (National first Professor Award). His present areas of research interest are the field of digital signal processing and communication.

Abbas Hasan Kattoush received his M.S. and Ph.D. degrees in communication engineering from USSR in 1979 and 1984, respectively. For 10 years Dr. Kattoush was a technical manager of a leading SAKHER computers company. He was a pioneer in computer networking and software engineering in Jordan. From 1993 to 2000 he worked at Applied Science University Amman Jordan where he was a founding member of the Department of Electrical and Computer Engineering. In 2000 Dr. Kattoush moved to Al-Isra University, Amman, Jordan. Currently he is an associate professor and a head of Department of Electrical and Computer Engineering, Al-Isra University. His areas of research interest include digital signal processing, digital communication systems, phase unwrapping, interferometric SAR image analysis, filtering, and interpretation. He has authored several tenths of research articles, textbooks, and computer software systems.

S.M. Abbas was born in 1951. He received his B.Sc. degree from Baghdad University in 1972, and his M.Sc. degree from Birmingham University in 1978. He is a lecturer in the Department of Electronic Engineering, College of Engineering, University of Baghdad in 1979, assistant professor in 1988. Currently he is the head of the Department of Electrical Engineering at University of Baghdad. His areas of research interest include fields in solid state electronics and communication engineering.

Ali T. Shaheen was born in Baghdad in 1978. He received his B.Sc. degree in electrical engineering from University of Baghdad in 2000, and his M.Sc. degree in electronic and communication from University of Baghdad 2007. He is working as a lecturer in the Electrical Engineering Department in the University of Baghdad. His areas of research interest are the field of digital signal processing and communication.